Discordance Between Histopathologic Grading and Dual-Tracer PET/CT Findings in Metastatic NETs and Outcome of ^{177}Lu-DOTATATE PRRT: Does In Vivo Molecular PET Perform Better from the Viewpoint of Prediction of Tumor Biology?

Aadil Adnan[1,2] and Sandip Basu[1,2]

[1]Radiation Medicine Centre, Bhabha Atomic Research Centre, Tata Memorial Hospital, Mumbai, India; and [2]Homi Bhabha National Institute, Mumbai, India

Discordance between histopathologic grading and dual-tracer PET/CT (^{68}Ga-DOTATATE and ^{18}F-FDG) findings in neuroendocrine tumors (NETs), though not typical, can be encountered in real-world scenarios. The aim of this study was to assess patients with discordance between World Health Organization (WHO) 2017 grade–predicted molecular PET/CT imaging and the actual dual-tracer PET/CT findings (by exploring their histopathologic, immunohistochemical, and molecular imaging characteristics), with a view toward identifying the prognostic determinants affecting outcome in a peptide receptor radionuclide therapy setup. **Methods:** Thirty-six patients with histopathologically proven inoperable, locally advanced or metastatic NETs, referred for peptide receptor radionuclide therapy, were included in this study. The cohort was divided into 2 broad population groups: those with discordance (between WHO 2017 grade–predicted molecular imaging and the dual-tracer PET/CT findings) and control (showing both ^{18}F-FDG and ^{68}Ga-DOTATATE uptake). The cohort was divided on the basis of dual-tracer PET/CT into 3 groups: metabolically inactive (non–[18]F-FDG-avid) and somatostatin receptor (SSTR)–expressing tumors, metabolically active (^{18}F-FDG-avid) and non–[68]Ga-DOTATATE-concentrating (non–SSTR-expressing) tumors, and matched imaging characteristics with the WHO 2017 grading system (showing both ^{18}F-FDG– and ^{68}Ga-DOTATATE–concentrating disease) for statistical analysis. Descriptive statistics were used to analyze categoric data; multivariate analysis was used to assess the correlation between different variables with progression-free survival (PFS) and overall survival (OS). Kaplan–Meier curves were used for survival analysis to calculate median survival and to analyze survival on the basis of WHO 2017 grading and dual-tracer PET. Cox proportional hazards regression analysis was used to determine predictors of survival (OS and PFS). **Results:** Of the 36-patient cohort, 24 (66.7%) showed discordance and 12 (33.3%) were in the control group. Among those showing discordance: 14 (38.9%) had metabolically inactive and SSTR-expressing disease and the remaining 10 (27.8%) had ^{18}F-FDG–concentrating and non–SSTR-expressing disease. Among those in the control group, 12 (33.3%) had intermediate-grade NETs and showed matched (^{68}Ga-DOTATATE– and ^{18}F-FDG–concentrating lesions) disease. Multivariate analysis in patients with discordant findings showed a significant correlation of dual-tracer PET with OS, whereas no significant correlation could be established between WHO grade and OS in the discordant subgroups. No significant correlation could be appreciated between PFS and either dual-tracer PET or WHO grading. The Kaplan–Meier analysis and Cox analysis showed dual-tracer PET/CT imaging to be a significant prognostic determinant and predictor of outcome, respectively. **Conclusion:** In NET patients with discordance between the 2 parameters, dual-tracer PET/CT with ^{18}F-FDG and ^{68}Ga-DOTATATE performed better than WHO grading, differentiation status, and immunohistochemistry in prognosticating and predicting outcome.

Key Words: neuroendocrine neoplasm; histopathologic grading; dual-tracer PET/CT; ^{68}Ga-DOTATATE; ^{177}Lu-DOTATATE; peptide receptor radionuclide therapy

Neuroendocrine neoplasms (NENs) are a heterogeneous group of widely distributed tumors comprising both neural and endocrine components (*1*). The neural component is based on identification of dense core granules, and the endocrine component refers to synthesis and secretion of monoamines. Histopathologic grading is considered to be the most important prognostic factor so far and helps in devising tailored therapeutic strategies for patients. However, confusion and enigma have always surrounded this approach, as outliers are quite noticeable in the day-to-day scenario.

Controversy has surrounded the entity since as early as the time that the term *carcinoid* (carcinoma-like) (*2*) was introduced by Oberndorfer at the start of the 20th century, because of the benign behavior of small-bowel tumors comprising argentaffin-positive argyrophilic cells (*3*). This term was criticized because of confusion regarding it and diagnostic irregularities and was regarded to be a misnomer, as these tumors displayed varying degrees of malignant potential (*4–6*). Later, a plethora of terms referring to neuroendocrine tumors (NETs)

was used, such as APUDoma, argentaffinoma, enteroendocrine tumors, tumors of diffuse endocrine system, and argyrophilic cell carcinoma. (7). In 1928, Masson characterized carcinoids as NETs on the basis of amine uptake and decarboxylation properties (8), whereas in 1963, Williams and Sandler classified them according to embryonic divisions of the digestive tract (5), and in 1972, Arrigoni et al. introduced the concept of typical and atypical based on histopathologic characteristics (9). In 1980, the World Health Organization (WHO) applied the term *carcinoid* to describe all NETs except pulmonary NETs (10); however, this usage led to more discord between pathologists and clinicians (11,12). In 1999, the Travis–WHO classification divided pulmonary and thymic NETs into typical carcinoid, atypical carcinoid, and large cell and small cell neuroendocrine carcinomas (NECs) (13–16). In 2000 and 2004, WHO revised the definition of gastroenteropancreatic and pulmonary/mediastinal NETs to reflect differentiation and mitotic index/necrosis, respectively (15,16). The WHO 2010 classification redefined the entire group of tumors as NENs and subdivided them according to proliferative index (Ki-67/MIB-1) and mitotic counts (17,18).

The 2010 WHO classification categorized NENs into 3 grades, with grades 1 and 2 referring to well-differentiated NETs and grade 3 (G3) referring to poorly differentiated NECs (17,18). In general, a well-differentiated NEN comprises cells showing minimal to moderate atypia, lacks necrosis, and expresses general markers of neuroendocrine differentiation (diffuse and intense synaptophysin and chromogranin A), whereas a poorly differentiated NEN comprises highly atypical small or large cells expressing faint neuroendocrine differentiation markers. In cases of discordance between differentiation and the proliferative index or when tumors do not concur with the predicted course, the National Comprehensive Cancer Network recommends that clinical judgment should trump the grading system (19). In cases of discrepancy between the proliferative and mitotic indices, the higher grade should prevail.

The 2010 WHO grading system was flawed in addressing the contrast between grade and differentiation. Although grade refers to the aggressiveness of tumor cells in terms of their potential for rapid growth and spread, differentiation is the morphologic resemblance of tumor cells to the islets of Langerhans (20,21). Hence, it was possible that well-differentiated NETs could be technically graded as G3 but might not be sensitive to the chemotherapy regimen used in poorly differentiated NECs (G3 NEC) (21). These well-differentiated NETs, which are technically classified as G3 NEC (on the basis of the proliferation index [WHO 2010]), may not be sensitive to the chemotherapy regimen indicated for G3 NECs. Interestingly, if an adequate number of pathologic specimens is available for an accurate mitotic count, most G3 NETs contain a proportion of cells with a mitotic rate of fewer than 20 per 10 high-power fields, and regions of a still lower grade may be present elsewhere in the tumor focus (20), hence rendering proliferation index and mitotic

counts to be focal rather than reflective of the overall tumor composition. Furthermore, the genomic composition of G3 NET resembles that of low-grade NET (i.e., MEN1, DAXX, and ATRX mutation) and differs distinctly from that of poorly differentiated NEC (i.e., p53 and RB1 mutation) (22). All these issues led to a revised WHO classification of NETs in 2017, which, along with its comparison to the 2010 WHO classification system, is detailed in Table 1 (23).

Furthermore, studies evaluating PET using ^{18}F-FDG and ^{68}Ga-DOTATATE showed a relatively lower ^{18}F-FDG concentration than did ^{68}Ga-DOTATATE in patients with G3 NEC—a finding contrary to that theoretically anticipated for G3 NEC on the basis of WHO 2010 (24). Receptor-targeted molecular imaging with PET/CT using ^{18}F-FDG and ^{68}Ga-DOTATATE provides an overall, semiquantitative assessment of tumor biology and burden. Hence, this use of dual tracers may potentially score over current conventional classification and grading systems, which rely mainly on focal needle sampling of the most accessible lesion (primary or metastatic) to guide the management strategy. The present study tried to evaluate the plausibility of this dual-tracer concept.

MATERIALS AND METHODS

Thirty-six patients (24 men [66.7%] and 12 women [33.3%]) with histopathologically proven NETs who had undergone peptide receptor radionuclide therapy (PRRT) at our center were retrospectively included in the study and their records analyzed. The median age for the cohort was 50 y (range, 25–66 y). The referral for PRRT was due to metastatic or inoperable locally advanced disease progressing on prior therapy (octreotide therapy or chemotherapy). Table 2 provides an overview of patient demographics.

The study was approved by our institutional scientific and medical ethics committee. The requirement to obtain informed consent was

TABLE 1
WHO NET Classification: 2010 vs. 2017 (23)

WHO classification	Ki-67 index	Mitoses/ 10 HPFs
2010		
Well-differentiated NENs		
NET G1	<3	<2
NET G2	3–20	2–20
Poorly differentiated NENs		
NEC G3 (small cell or large cell)	>20	>20
MANEC		
2017		
Well-differentiated NENs		
NET G1	<3	<2
NET G2	3–20	2–20
NET G3	>20	>20
Poorly differentiated NENs		
NEC G3	>20	>20
Small cell type		
Large cell type		
MiNEN		

HPF = high-power field.

TABLE 2
Patient Demographics

Demographic	Data
Total patients	36 (100%)
Sex	
Male	24 (67%)
Female	12 (33%)
Age (y)	
Median	50
Range	25–66
Site of primary	
Pancreas	12 (33.3%)
Unknown	7 (19.4%)
Rectum	5 (13.9%)
Small bowel	4 (11.1%)
Lung	3 (8.3%)
Mediastinum	2 (5.6%)
Stomach	1 (2.8%)
Gallbladder	1 (2.8%)
Skin appendages (Merkel cell carcinoma)	1 (2.8%)
WHO grade (2017 classification)	
G1 NET	7 (19.4%)
G2 NET	15 (41.7%)
G3 NET	7 (19.4%)
G3 NEC	7 (19.4%)
Differentiation status	
Well-differentiated	27 (75.0%)
Poorly differentiated	7 (19.4%)
Not known	2 (5.6%)

Data are number and percentage, except for age.

waived because these patients were referred for PRRT, and the ^{18}F-FDG and ^{68}Ga-DOTATATE scans were done as a part of the routine pretherapy workup. The patients were categorized on the basis of the current 2017 WHO classification. The cohort was divided into 2 broad groups: those with discordance (between WHO 2017 grade–predicted dual-tracer PET/CT findings and the actual dual-tracer PET/CT findings) and a control group (showing both ^{18}F-FDG and ^{68}Ga-DOTATATE uptake). The cohort was divided on the basis of dual-tracer PET into metabolically inactive (non–^{18}F-FDG-avid) and somatostatin receptor (SSTR)–expressing, metabolically active (^{18}F-FDG–avid) and non–SSTR-expressing, and matched (showing both metabolic activity and SSTR expression) and according to the WHO 2017 grading system for statistical analysis. An SUV_{max} of 2.5 on ^{18}F-FDG PET/CT was standardized to an SUV_{max} of 9.0 on ^{68}Ga-DOTATATE PET/CT. The inclusion criteria were histopathologically proven NET/NEC and discordance between histopathologic (WHO 2017) grade–predicted dual-tracer PET and actual dual-tracer PET findings.

All statistical analyses were performed by SPSS software, version 23.0 (SPSS Inc.). Descriptive statistics were used to analyze categoric data. Multivariate analysis was used to evaluate the correlation of different variables with progression-free survival (PFS) and overall survival (OS). The Kaplan–Meier product limit method was used to calculate median survival and to analyze survival on the basis of WHO 2017 grade and dual-tracer PET. The variables dual-tracer PET and WHO 2017 grade determining OS and PFS were compared using the log-rank test. Cox proportional hazards regression analysis was used to identify predictors of OS and PFS. Patients who were

alive or with nonprogressive disease (for OS and PFS, respectively) at the time of analysis or last contact were censored. A 2-tailed P value of less than 0.05 was considered statistically significant, and hazard ratios with 95% CIs were determined.

RESULTS

The pancreas was the most commonly involved primary site (12 patients, 33.3%), followed by unknown primary (7 patients, 19.4%), rectum (5 patients, 13.9%), small bowel (4 patients, 11.1%), lungs (3 patients, 8.3%), mediastinum (2 patients, 5.6%), and stomach, gallbladder, and skin appendages (Merkel cell carcinoma), each with a single patient (2.8%). According to the 2017 WHO grading, 15 patients (41.7%) had grade 2 (G2) NET, followed by 7 patients (19.4%) each with grade 1 (G1) NET, G3 NET, and G3 NEC. Twenty-four patients (66.7%) were in the discordance group, and 12 (33.3%) were in the control group. In the discordance group, 14 patients (38.9%) had metabolically inactive and SSTR-expressing disease, and the remaining 10 (27.8%) had metabolically active and non–SSTR-expressing disease. In the control group, all 12 patients (33.3%) and intermediate-grade NETs and showed matched (metabolically active and SSTR-expressing) disease.

Twenty-seven patients (75%) had a well-differentiated histology, 7 (19.4%) had a poorly differentiated histology, and in 2 (5.6%) the histology was not available. Thirty patients (83.3%) were synaptophysin-positive, and in remaining 6 (16.7%) the data were unavailable. Twenty-six patients (72.2%) were positive for chromogranin A, 3 were negative (8.3%), and in remaining 7 (19.4%) the data were unavailable. However, no definitive pattern could be established in chromogranin A–negative patients. Similarly, no definitive trend or pattern was appreciated between epithelial or other immunohistochemistry (IHC) markers and other variables, as possibly could be due in part to inconsistent selection of IHC markers in patients and hence lack of uniformity (Table 3).

TABLE 3
Histopathologic Characteristics

Characteristic	Data
Synaptophysin (IHC)	
Positive	30 (83.3%)
Negative	6 (16.7%)
Chromogranin A (IHC)	
Positive	26 (72.2%)
Negative	3 (8.3%)
Not known	7 (19.4%)
Epithelial markers (AE1/AE3; IHC)	
Positive	11 (30.6%)
Negative	2 (5.6%)
Not known	23 (63.9%)
Other IHC markers (ATRX, cytokeratin, CD56, CK7, CK19, CK20, and CDX2)	
Positive	10 (27.8%)
Not known	26 (72.2%)

Data are number and percentage.

Of the 24 patients with discordant NET (in terms of WHO grade–predicted and actual dual-tracer PET findings), 7 (~30%) progressed (2/14 [14.3%] with metabolically inactive and SSTR-expressing disease and 5/10 [50%] with metabolically active and non–SSTR-expressing disease) and 8 (~33.3%) succumbed to the disease (1/14 [7.1%] with metabolically inactive and SSTR-expressing disease and 7/10 [70%] with metabolically active and non–SSTR-expressing disease). Of the 12 control patients with matched disease, 3 (25%) progressed and 5 (41.7%) died. In the entire cohort, the median cumulative PFS was 83 mo (82.9 mo for metabolically inactive and SSTR-expressing and 49.8 mo for metabolically active and non–SSTR-expressing) and OS was 118 mo (90 mo for metabolically inactive and SSTR-expressing and 61.2 mo for metabolically active and non–SSTR-expressing). Categorization based on WHO 2017 grading did not yield such trends and results (Figs. 1 and 2). The dual-tracer PET/CT characteristics of the patient population has been detailed in Table 4.

On multivariate analysis, the only significant correlation was between dual-tracer PET and OS ($P = 0.01$); however, no significant correlation was flagged between any of the variables and PFS in this study.

For PFS and OS, dual-tracer PET and WHO 2017 grading were compared by Kaplan–Meier analysis and plots (Figs. 1 and 2). A significant difference was noticed between the Kaplan–Meier plots when categorization was based on dual-tracer PET ($P = 0.05$ for PFS and $P = 0.02$ for OS; log rank test) versus WHO 2017 grading ($P = 0.39$ for PFS and 0.67 for OS; log rank test). Cox analysis was used to analyze dual-tracer PET versus WHO 2017 grading as a predictor of PFS and OS and showed dual-tracer imaging to be an independent predictive prognostic variable (PFS: hazard ratio, 0.23 [95% CI, 0.31–1.67; $P = 0.03$]; OS: hazard ratio, 0.027 [95% CI, 0.002–0.35; $P = 0.005$]). No significant statistics could be achieved for WHO 2017 grading (PFS: hazard ratio, 0.49 [95% CI, 0.061–3.861; $P = 0.5$]; OS: hazard ratio, 0.301 [95% CI, 0.3–3.013; $P = 0.31$]).

A smaller substudy was done categorizing patients on the basis of ^{68}Ga-DOTATATE uptake (Krenning score). Two patients ($n = 2$) with a Krenning score of 1 were denied PRRT. Of 5 patients with a Krenning score of 2, 2 received a single cycle of PRRT and the remaining 3 received 2–3 cycles (with the first cycle given mainly on trial or compassionate-use grounds because there were few available alternatives). Additional PRRT cycles in Krenning 2 patients were administered either because of some initial symptomatic benefit or as part of a combined chemo-PRRT trial, which in almost all cases showed—after a third cycle of PRRT—disease progression, which was followed by withholding of further PRRT. Of 7 patients with a Krenning score of 1 or 2, 5 (71.4%) progressed and all 7 (100%) succumbed to disease with an adverse clinical outcome (marked by a relatively brief OS and PFS). The cohort with a Krenning score of 3 or 4 comprised 29 patients (80.6%), of whom 10 (27.8%) and 19 (52.8%) had a Krenning score of 3 and 4, respectively. Of these 29 patients, 5 (17.2%) progressed and 6 (20.7%) died. Hence, a higher SSTR expression was associated with a favorable outcome and vice versa.
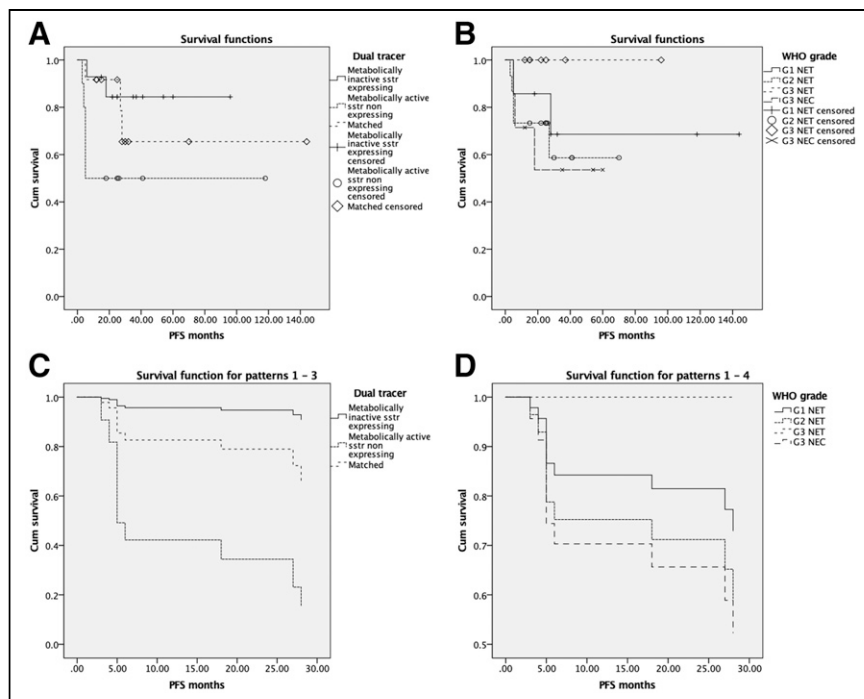
DISCUSSION

The WHO 2010 grading system was revised in 2017 to classify NETs with a Ki-67 of more than 20% as well-differentiated and NECs with a Ki-67 of more than 20% as poorly differentiated. (Earlier in 2010 grading, all NETs with Ki-67 > 20% were considered NEC.) Ideally, grade I NETs should have high ^{68}Ga-DOTATATE uptake and low ^{18}F-FDG uptake, and grade III NETs and NECs should have low

FIGURE 1. (A) Kaplan–Meier curves for PFS on basis of dual-tracer PET. (B) Kaplan–Meier curves for PFS on basis of 2017 WHO grading system. (C) Cox proportional hazards survival curves for PFS on basis of dual-tracer PET. (D) Cox proportional hazards survival curves for PFS on basis of 2017 WHO grading system. Kaplan–Meier and Cox curves showed significantly better PFS for metabolically inactive and SSTR-expressing group than for metabolically active and non–SSTR-expressing group when cohort was analyzed on basis of dual-tracer PET. Analysis based on 2017 WHO grading system did not yield any significant difference. Cum = cumulative.
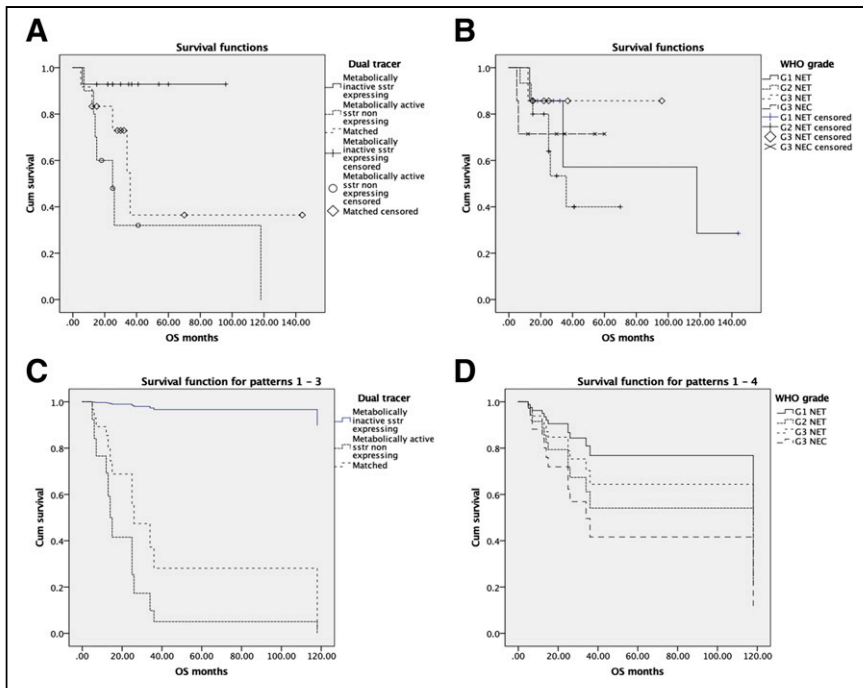
FIGURE 2. (A) Kaplan–Meier curves for OS on basis of dual-tracer PET. (B) Kaplan–Meier curves for OS on basis of 2017 WHO grading system. (C) Cox proportional hazards survival curves for OS on basis of dual-tracer PET. (D) Cox proportional hazards survival curves for OS on basis of 2017 WHO grading system. Kaplan–Meier and Cox curves showed significantly better OS for metabolically inactive and SSTR-expressing group than for metabolically active and non–SSTR-expressing group when cohort was analyzed on basis of dual-tracer PET. Analysis based on 2017 WHO grading system did not yield any significant difference. Cum = cumulative.

^{68}Ga-DOTATATE uptake and high ^{18}F-FDG uptake. But our clinical experience has shown obvious outliers with high ^{18}F-FDG uptake and low ^{68}Ga-DOTATATE uptake in grade I NETs and vice versa (high ^{68}Ga-

TABLE 4
Dual-Tracer PET Characteristics

Characteristic	Data
Baseline ^{18}F-FDG uptake (SUV$_{max}$)	
<5	14 (38.9%)
5–10	5 (13.9%)
10–20	10 (27.8%)
>20	7 (19.4%)
Baseline DOTATATE uptake	
Krenning 1	2 (5.6%)
Krenning 2	5 (13.9%)
Krenning 3	10 (27.8%)
Krenning 4	19 (52.8%)
Dual-tracer PET	
Metabolically inactive and SSTR-expressing	14 (38.9%)
Metabolically active and non–SSTR-expressing	10 (27.8%)
Matched (metabolically active and SSTR-expressing)	12 (33.3%)

Data are number and percentage.

DOTATATE uptake and low ^{18}F-FDG uptake in grade III NETs and NECs). Grade II NETs have shown mixed uptake. Usually, histopathologic grading serves as an excellent prognostic marker, and in most cases, the functional imaging findings are in concordance with it. But when there is discordance, histopathologic grading may not reflect the exact, overall tumor biology, as clinically observed and affirmed by this study.

Here, we specifically evaluated NETs showing discordance between actual functional imaging findings (^{68}Ga-DOTATATE and ^{18}F-FDG) and imaging findings predicted by 2017 WHO grade. These entities, although not regularly encountered in normal clinical scenarios, do exist. The study group comprised patients with contradictory imaging findings (e.g., ^{68}Ga-DOTATATE–negative and ^{18}F-FDG–positive findings in grade I well-differentiated tumors and vice versa). We tried to evaluate and explain this paradoxic behavior of some NETs and whether dual-tracer PET/CT can aid in therapeutic decision making and predict the outcome of treatment, especially PRRT. The main objective of this study was to evaluate the validity of dual-tracer PET/CT as a prognostic marker in comparison to other available determinants (e.g., histopathology), especially in deciding whether PRRT is a therapeutic option and in predicting its outcome. This concept resonated with the WHO's approach in classifying G3 NETs as well differentiated (G3 NET) or poorly differentiated (G3 NEC), exhibiting a stark contrast in their biologic behavior and response to treatment (particularly chemotherapy) and ultimately culminating in the current 2017 WHO NET grading system.

This nuanced difference from the usual and predicted course may be secondary to high-grade transformation of original low-grade disease, as well as to overestimation and generalization of histopathologic and IHC findings as representative of the tumor or the overall disease burden, whereas such findings essentially are—in most if not all cases—a localized and focal representation covering the extent of only the sampling needle tip or the tissue specimen biopsied. Vis-à-vis discordant NETs, the current database of available articles is relatively deficient, with only occasional reports, and these are both nascent and ambiguous in their understanding of the entity. Tang et al., in their study of the histopathologic, IHC, and genetic constitution of well-differentiated NETs (25), deduced that mixed grades do exist within the population of well-differentiated NETs and are distinguishable from poorly differentiated NECs by their

unique phenotype, proliferative indices, and genotype, either at the time of diagnosis or afterward at both primary and metastatic sites. Nuñez-Valdovinos et al., in a study using the large Spanish tumor registry (RGETNE [Registro del Grupo Español de Tumores Neuroendocrinos]) (26), inferred that substantial clinical heterogeneity is observed for both G2 and G3 NENs and that analysis of the tumor registry suggested tumor morphology to be a valuable aid in addition to the proliferation index, to further stratify the clinical outcome and prognosis in patients with gastroenteropancreatic NENs. Choe et al., in their review article (22), highlighted that functional imaging—specifically, SSTR scintigraphy (SRS with ^{68}Ga-DOTATATE) and ^{18}F-FDG—may be helpful in distinguishing well-differentiated NETs from poorly differentiated NECs (27), especially in challenging situations with a discrepancy between imaging features and histology. In the context of NECs, which do not always show positive IHC markers (28), or when a tissue sample may not be representative of the entire tumor or disease burden, functional imaging with dual-tracer PET has a particularly important role to play (29). Basu et al. (24) also concluded that even in the presence of different proliferative indices, an inverse correlation in uptake on ^{68}Ga-DOTATATE and ^{18}F-FDG PET is propitious in 3 instances: cases requiring in vivo depiction of the overall tumor phenotype resulting from multiple putative and unknown interactions at the cellular level; cases involving interlesional and intralesional heterogeneity, rendering histopathology and IHC subject to possible sampling errors and underrepresentation; and cases requiring assessment of tumor biology using intermediate grading indices. Thapa et al. (30) and Zhang et al. (31) showed that high ^{18}F-FDG uptake was associated with poorer outcomes in NETs treated with PRRT. However, symptomatic improvement was observed in most cases irrespective of grade and ^{18}F-FDG uptake. High pretherapy ^{18}F-FDG uptake in both low-grade and high-grade NETs predicted an inferior outcome and was associated with disease progression. Although these studies emphasize the prognostic implication of ^{18}F-FDG uptake, the study by Thapa et al. used the WHO 2010 NET grading system and did not take into account the value of dual-tracer PET, and neither study evaluated the discordance between actual functional imaging findings and histopathologic grade–predicted dual-tracer functional PET findings. The literature data make clear that both ^{18}F-FDG and ^{68}Ga-DOTATATE uptake would form determinants of response and that their relative concentrations on PET/CT imaging would be an important molecular imaging parameter for such predictions (32–35). In a previously published study from our center (36), Sampathirao et al. investigated the potential role of dual-tracer PET/CT in detection of the primary site in carcinoma of unknown primary, and the findings on PET/CT usually correlated well with the tumor proliferation index; however, a few outliers were noticed. Some of these outliers may have been included in the present study, which looked primarily into their outcome viewpoint (clinical response to PRRT/chemotherapy).

For such clinical situations, imaging using dual tracers has proved useful, as individual sampling of all lesions will be almost impossible for obvious practical and ethical reasons. Dual-tracer ^{68}Ga-DOTATATE and ^{18}F-FDG imaging seems potentially advantageous and pragmatic for several reasons: it can provide a noninterventional representation of whole-body disease burden; it shows relative tracer uptake reflective of differentiation status and lesion aggressiveness; it can direct the appropriate treatment strategy; it is effective in evaluating responses and determining prognoses; and, to a lesser extent, it can guide toward the diagnosis (Figs. 3 and 4). The present study was unique in that it evaluated a small and specified entity: discordance between WHO 2017 grade–predicted dual-tracer PET/CT findings and the actual dual-tracer PET/CT findings. There were encouraging results supporting the role of dual-tracer functional imaging in solving the conundrum surrounding management and prognosis, and the study was imperative in its concept and approach. The PFS and OS of the patients with discordance correlated more closely with the dual-tracer PET findings as opposed to the 2017 WHO grading system. Furthermore, dual-tracer PET (as opposed to the 2017 WHO grading) was found to be an independent prognostic factor for PFS and OS.
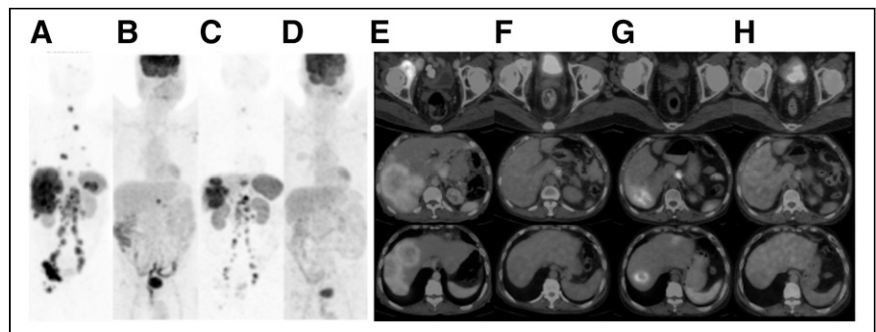

FIGURE 3. A 61-y-old man with NET metastatic to liver, mediastinal and abdominal nodes, and multiple skeletal sites, with unknown primary. Histopathology revealed poorly differentiated NEC, positive for synaptophysin and chromogranin, and CK19-positive on IHC. Despite high proliferative index of 25%, ^{68}Ga-DOTATATE PET/CT at baseline revealed intense SSTR expression in hepatic and skeletal lesions and in mediastinal, abdominal, and pelvic nodes, whereas ^{18}F-FDG PET/CT showed single metabolically active pariceliac node. Follow-up ^{68}Ga-DOTATATE PET/CT revealed partial response, with decrease in size and SSTR expression in almost all lesions, whereas ^{18}F-FDG PET/CT did not show any abnormal uptake, suggesting complete metabolic resolution. Despite poorly differentiated G3 NEC (WHO 2017), dual-tracer PET/CT studies suggested favorable tumor biology, which was adequately clinically translated. After third PRRT, patient is doing fine, with significant symptomatic and morphologic improvement.
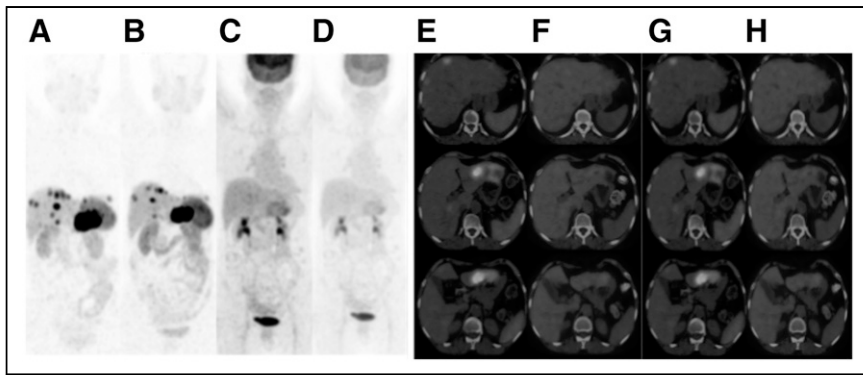
FIGURE 4. A 64-y-old woman with NET metastatic to liver and skeletal sites, with unknown primary. Patient presented with pain in abdomen and weight loss and was referred for PRRT in view of SSTR-expressing metastatic NET. Histopathology of liver lesion revealed metastatic, well-differentiated NET with MIB-1 index of 24%, positive for synaptophysin and chromogranin, and CDX2-negative on IHC. Baseline ^{68}Ga-DOTATATE PET/CT revealed multiple areas of increased tracer uptake (SSTR expression) in both lobes of liver (bilobar hepatic metastases, which is not amenable to surgical resection) and skeletal sites, with no abnormal hypermetabolism evident on baseline ^{18}F-FDG PET/CT. Follow-up dual-tracer PET/CT after 4 PRRTs showed decrease in number of smaller hepatic metastases, with mild interval decrease in size of larger hepatic lesion in left lobe (overall partial response). Dual-tracer PET/CT appeared to agree with histopathologic finding of well-differentiated G3 NET (WHO 2017), and findings were adequately clinically translated.

The major limitations of the study were its retrospective design, its lack of a homogeneous histopathology protocol (especially with respect to IHC markers), and its lack of a standardized approach to tumor marker evaluation among the referring institutions and hospitals. Another possible limitation was that the cohort lacked uniformity in disease burden and general condition, which could affect the duration of OS and PFS in these heavily pretreated patients, who had been referred for PRRT at various disease stages. The fact that genetic mutations and pathways were not studied might represent a major pitfall that we believe could be pivotal to discordance. An understanding of such mutations and pathways could potentially lead to a paradigm shift in our present management of discordant NETs. However, this study did have some important findings. In evaluating the novel concept of discordance between WHO 2017 grade–predicted molecular imaging and actual dual-tracer PET/CT findings, it showed encouraging results in favor of dual-tracer PET. It highlighted possible pitfalls in histopathologic grading and its reliability in devising a personalized treatment strategy. It revealed the need for a well-structured prospective study recruiting a homogeneous patient cohort. Finally, it showed that the greatest need in deciphering this medical conundrum is to perform studies encompassing all possible determinants, including genomic and proteomic analyses.

CONCLUSION

Dual-tracer PET using ^{18}F-FDG and ^{68}Ga-DOTATATE is a promising entity in NET management and may perform better than histopathology in evaluating overall tumor burden and biology, especially in making clinical decisions and selecting patients who will benefit from PRRT. The present work indicated that histologic classification alone is not sufficient. On

the one hand, a focal high MIB-1 index should not preclude a patient from PRRT (if SSTR PET imaging reveals high receptor expression), and on the other hand, a low tumor proliferation rate at initial diagnosis does not clearly predict concordant biology in all lesions. Because a temporal change in tumor grade (dedifferentiation) is possible, a workup that includes the dual-tracer PET/CT features would be useful and add a scientific basis to the management strategy. Discordance in NETs can be multifaceted and complex, for which a continued multidisciplinary approach is the key to gaining greater insight.

DISCLOSURE

No potential conflict of interest relevant to this article was reported.

KEY POINTS

QUESTION: How does the issue of discordance between histopathologic grading and dual-tracer PET/CT (^{68}Ga-DOTATATE and ^{18}F-FDG) findings in metastatic NENs affect routine clinical practice?

PERTINENT FINDINGS: Dual-tracer PET/CT imaging was shown to be a significant prognostic determinant and predictor of outcome.

IMPLICATIONS FOR PATIENT CARE: A multifaceted workup encompassing dual-tracer PET/CT features along with histopathology would be greatly useful and add scientific basis to the management strategy.

REFERENCES

1. Basu B, Sirohi B, Corrie P. Systemic therapy for neuroendocrine tumours of gastroenteropancreatic origin. *Endocr Relat Cancer.* 2010;17:R75–R90.
2. Modlin IM, Shapiro MD, Kidd M. Siegfried Oberndorfer: origins and perspectives of carcinoid tumors. *Hum Pathol.* 2004;35:1440–1451.
3. Rosai J. The origin of neuroendocrine tumors and the neural crest saga. *Mod Pathol.* 2011;24(suppl):S53–S57.
4. Modlin IM, Sandor A. An analysis of 8305 cases of carcinoid tumors. *Cancer.* 1997;79:813–829.
5. Williams ED, Sandler M. The classification of carcinoid tumours. *Lancet.* 1963;1:238–239.
6. Soga J. The term "carcinoid" is a misnomer: the evidence based on local invasion. *J Exp Clin Cancer Res.* 2009;28:15.
7. Hajdu SI, Tang P. A note from history: the saga of carcinoid and oat-cell carcinoma. *Ann Clin Lab Sci.* 2008;38:414–417.
8. Masson P. Carcinoids (argentaffin-cell tumors) and nerve hyperplasia of appendicular mucosa. *Am J Pathol.* 1928;4:181–212.
9. Arrigoni MG, Woolner LB, Bernatz PE. Atypical carcinoid tumors of the lung. *J Thorac Cardiovasc Surg.* 1972;64:413–421.
10. Williams ED. *Histological Typing of Endocrine Tumours.* Geneva: Springer; 1980.
11. Chang S, Choi D, Lee SJ, et al. Neuroendocrine neoplasms of the gastrointestinal tract: classification, pathologic basis, and imaging features. *Radiographics.* 2007;27:1667–1679.

12. Vinik A, Hughes MS, Feliberti E, et al. Carcinoid tumors. National Center for Biotechnology Information website. http://www.ncbi.nlm.nih.gov/books/NBK279162/. Updated February 5, 2018. Accessed March 25, 2022.

13. Pusceddu S, Catena L, Valente M, et al. Long-term follow up of patients affected by pulmonary carcinoid at the Istituto Nazionale Tumori of Milan: a retrospective analysis. *J Thorac Dis.* 2010;2:16–20.

14. Axiotis CA. The neuroendocrine lung. In: Li Volsi V, Asa SL, eds. *Endocrine Pathology.* Churchill Livingstone; 2002:261–296.

15. Klöppel G. Classification and pathology of gastroenteropancreatic neuroendocrine neoplasms. *Endocr Relat Cancer.* 2011;18(suppl 1):S1–S16.

16. Travis WD. The concept of pulmonary neuroendocrine tumours. In: Travis WD, Brambilla E, Muller-Hermelink HK, Harris CC, eds. *Pathology and Genetics of Tumours of the Lung, Pleura, Thymus and Heart.* IARC Press; 2004:59–64.

17. Farrell JM, Pang JC, Kim GE, Tabatabai ZL. Pancreatic neuroendocrine tumors: accurate grading with Ki-67 index on fine-needle aspiration specimens using the WHO 2010/ENETS criteria. *Cancer Cytopathol.* 2014;122:770–778.

18. Bosman FT, Carneiro F, Hruban RH, Theise ND. *WHO Classification of Tumours of the Digestive System.* 4th ed. International Agency for Research on Cancer; 2010.

19. Neuroendocrine tumors guidelines. Medscape website. http://emedicine.medscape.com/article/2500010-overview. Updated July 27, 2020. Accessed March 25, 2022.

20. Singhi AD, Klimstra DS. Well-differentiated pancreatic neuroendocrine tumours (PanNETs) and poorly differentiated pancreatic neuroendocrine carcinomas (PanNECs): concepts, issues and a practical diagnostic approach to high-grade (G3) cases. *Histopathology.* 2018;72:168–177.

21. Klimstra DS, Modlin IR, Coppola D, Lloyd RV, Suster S. The pathologic classification of neuroendocrine tumors: a review of nomenclature, grading, and staging systems. *Pancreas.* 2010;39:707–712.

22. Choe J, Kim KW, Kim HJ, et al. What is new in the 2017 World Health Organization classification and 8th American Joint Committee on Cancer staging system for pancreatic neuroendocrine neoplasms? *Korean J Radiol.* 2019;20:5–17.

23. Lloyd RV, Osamura RY, Klöppel G, Rosai J. *WHO Classification of Tumours of Endocrine Organs.* 4th ed. International Agency for Research on Cancer; 2017: 209–240.

24. Basu S, Ranade R, Thapa P. Correlation and discordance of tumour proliferation index and molecular imaging characteristics and their implications for treatment decisions and outcome pertaining to peptide receptor radionuclide therapy in patients with advanced neuroendocrine tumour. *Nucl Med Commun.* 2015;36:766–774.

25. Tang LH, Untch BR, Reidy DL, et al. Well-differentiated neuroendocrine tumors with amorphologically apparent high-grade component: a pathway distinct from poorly differentiated neuroendocrine carcinomas. *Clin Cancer Res.* 2016;22:1011–1017.

26. Nuñez-Valdovinos B, Carmona-Bayonas A, Jimenez-Fonseca P, et al. Neuroendocrine tumor heterogeneity adds uncertainty to the World Health Organization 2010 classification: real-world data from the Spanish tumor registry (R-GETNE). *Oncologist.* 2018;23:422–432.

27. Rust E, Hubele F, Marzano E, et al. Nuclear medicine imaging of gastroentero-pancreatic neuroendocrine tumors: the key role of cellular differentiation and tumor grade—from theory to clinical practice. *Cancer Imaging.* 2012;12:173–184.

28. Lam KY, Lo CY. Pancreatic endocrine tumour: a 22-year clinico-pathological experience with morphological, immunohistochemical observation and a review of the literature. *Eur J Surg Oncol.* 1997;23:36–42.

29. Volante M, Righi L, Berruti A, Rindi G, Papotti M. The pathological diagnosis of neuroendocrine tumors: common questions and tentative answers. *Virchows Arch.* 2011;458:393–402.

30. Thapa P, Ranade R, Ostwal V, Shrikhande SV, Goel M, Basu S. Performance of ^{177}Lu-DOTATATE-based peptide receptor radionuclide therapy in metastatic gastroenteropancreatic neuroendocrine tumor: a multiparametric response evaluation correlating with primary tumor site, tumor proliferation index, and dual tracer imaging characteristics. *Nucl Med Commun.* 2016;37:1030–1037.

31. Zhang J, Liu Q, Singh A, Schuchardt C, Kulkarni HR, Baum RP. Prognostic value of ^{18}F-FDG PET/CT in a large cohort of patients with advanced metastatic neuroendocrine neoplasms treated with peptide receptor radionuclide therapy. *J Nucl Med.* 2020;61:1560–1569.

32. Basu S, Chakraborty S, Parghane RV. et al. One decade of 'bench-to-bedside' peptide receptor radionuclide therapy with indigenous [^{177}Lu]Lu-DOTATATE obtained through 'direct' neutron activation route: lessons learnt including practice evolution in an Indian setting. *Am J Nucl Med Mol Imaging.* 2020;10:178–211.

33. Basu S, Parghane RV, Kamaldeep CS. Peptide receptor radionuclide therapy of neuroendocrine tumors. *Semin Nucl Med.* 2020;50:447–464.

34. Sitani K, Parghane RV, Talole S, Basu S. Long-term outcome of indigenous ^{177}Lu-DOTATATE PRRT in patients with metastatic advanced neuroendocrine tumours: a single institutional observation in a large tertiary care setting. *Br J Radiol.* 2021;94:20201041.

35. Adnan A, Sampathirao N, Basu S. Implications of fluorodeoxyglucose uptake in low-intermediate grade metastatic neuroendocrine tumors from peptide receptor radionuclide therapy outcome viewpoint: a semi-quantitative standardized uptake value-based analysis. *World J Nucl Med.* 2019;18:389–395.

36. Sampathirao N, Basu S. MIB-1 index-stratified assessment of dual-tracer PET/CT with ^{68}Ga-DOTATATE and ^{18}F-FDG and multimodality anatomic imaging in metastatic neuroendocrine tumors of unknown primary in a PRRT workup setting. *J Nucl Med Technol.* 2017;45:34–41.